THE JOURNAL OF BIOLOGICAL CHEMISTRY VOL. 286, NO. 14, pp. 12702–12711, April 8, 2011

A Dominant-negative Gα Mutant That Traps a Stable Rhodopsin-Gα-GTP-βγ Complex*

Received for publication, July 21, 2010, and in revised form, December 16, 2010 Published, JBC Papers in Press, February 1, 2011, DOI 10.1074/jbc.M110.166538

Sekar Ramachandran and Richard A. Cerione[1]

From the Department of Chemistry and Chemical Biology and Department of Molecular Medicine, Cornell University, Ithaca, New York 14853

Residues comprising the guanine nucleotide-binding sites of the α subunits of heterotrimeric (large) G-proteins (Gα subunits), as well as the Ras-related (small) G-proteins, are highly conserved. This is especially the case for the phosphate-binding loop (P-loop) where both Gα subunits and Ras-related G-proteins have a conserved serine or threonine residue. Substitutions for this residue in Ras and related (small) G-proteins yield nucleotide-depleted, dominant-negative mutants. Here we have examined the consequences of changing the conserved serine residue in the P-loop to asparagine, within a chimeric Gα subunit (designated α_T*) that is mainly comprised of the α subunit of the retinal G-protein transducin and a limited region from the α subunit of Gi1. The α_T*(S43N) mutant exhibits a significantly higher rate of intrinsic GDP-GTP exchange compared with wild-type α_T*, with light-activated rhodopsin (R*) causing only a moderate increase in the kinetics of nucleotide exchange on α_T*(S43N). The α_T*(S43N) mutant, when bound to either GDP or GTP, was able to significantly slow the rate of R*-catalyzed GDP-GTP exchange on wild-type α_T*. Thus, GTP-bound α_T*(S43N), as well as the GDP-bound mutant, is capable of forming a stable complex with R*. α_T*(S43N) activated the cGMP phosphodiesterase (PDE) with a dose-response similar to wild-type α_T*. Activation of the PDE by α_T*(S43N) was unaffected if either R* or β1γ1 alone was present, whereas it was inhibited when R* and the β1γ1 subunit were added together. Overall, our studies suggest that the S43N substitution on α_T* stabilizes an intermediate on the G-protein activation pathway consisting of an activated G-protein-coupled receptor, a GTP-bound Gα subunit, and the β1γ1 complex.

G protein-coupled receptors (GPCR)[2] are one of the largest families of membrane proteins and are involved in various physiological functions. In the past several years, significant advances have been made in the determination of structures at an atomic level of GPCRs (1, 2), their cognate G-proteins, and their downstream targets (3). In addition, structures have been solved for complexes of G-proteins with their downstream targets as well as their regulators (*e.g.* the regulators of G-protein signaling (RGS) proteins) (3). However, one of the central unresolved questions in this field involves the mechanism utilized by a GPCR to catalyze the release of GDP from its cognate G-protein (4, 5).

The x-ray crystal structures of various Gα subunits have shown that they are composed of two distinct domains: one that highly resembles the GTPase domain of the small G-protein Ras, and a second domain which is mainly α-helical in content and thus referred to as the helical domain. The guanine nucleotide is nestled between these two domains (4, 5). The binding of GTP to α_T induces structural changes within 3 regions of the GTPase domain, designated as Switches 1, 2, and 3.

The vertebrate visual system in rod cells has provided an excellent model system for understanding how GPCRs activate heterotrimeric G-proteins and subsequently their downstream targets (6, 7). In the visual transduction pathway, the absorption of a photon leads to the isomerization of the covalently-bound chromophore, 11-*cis*-retinal, to its all-*trans* configuration. This converts rhodopsin to its functionally active conformation referred to as metarhodopsin II (R*). The heterotrimeric G-protein transducin is made up of a GDP-bound α subunit (α_T-GDP), as well as the β1 and γ1 subunits, which are noncovalently complexed to each other and can be dissociated only by denaturation. The R* species binds to heterotrimeric transducin (α_T-GDP/β1γ1) with an extremely high affinity. This results in a weakening of the affinity of α_T for GDP such that it dissociates from the G-protein. GTP then binds to α_T yielding a species (α_T-GTP) that has a reduced affinity for both R* and β1γ1. The structural changes in the switch regions of α_T-GTP allow it to bind and activate the downstream effector enzyme, the cGMP phosphodiesterase (PDE). The PDE is made up of two catalytic subunits (α_{PDE} and β_{PDE}) and two smaller regulatory subunits (γ_{PDE}) and catalyzes the rapid hydrolysis of cGMP to GMP. The α_T-GTP species binds to γ_{PDE} and relieves its inhibition of the catalytic activity of the α_{PDE} and β_{PDE} subunits. The activation of PDE is terminated by the hydrolysis of GTP by α_T, which is catalyzed by RGS9. The conversion of cGMP to GMP leads to a closure of cGMP-gated channels on the rod cell membrane. This hyperpolarization results in an inhibition of neurotransmitter release, which represents the signal that is conveyed to the optic nerve.

Our laboratory has been interested in identifying and biochemically characterizing α_T mutants that might help to shed light on the mechanism by which GDP is released from a Gα subunit, thus leading to G-protein activation (8–12). These

* This work was supported, in whole or in part, by National Institutes of Health Grant GM047458.

[1] To whom correspondence should be addressed: Dept. of Molecular Medicine, Cornell University, Ithaca, NY 14853-6401. Tel.: 607-253-3888; Fax: 607-253-3659; E-mail: rac1@cornell.edu.

[2] The abbreviations used are: GPCR, G protein-coupled receptor; PDE, cGMP-phosphodiesterase; cGMP, cyclic guanosine monophosphate; GTPγS, guanosine-5′-*O*-(3-thiotriphosphate); ROS, rod outer segment; HPLC, high pressure liquid chromatography; P-loop, phosphate-binding loop; AlF_4^-, aluminum fluoride; Gpp(NH)p, guanosine 5′-(β,γ-imido)triphosphate.

efforts have resulted in the identification of various Gα mutants with novel biochemical properties. Owing to the difficulties in overexpressing native α_T in *Escherichia coli*, we have used a chimera of α_T and α_{i1}, referred to as α_T*, as a starting Gα-backbone for these studies (13).

G-proteins belonging to both the monomeric (small) and heterotrimeric (large) G-protein families have a conserved serine or threonine residue in the P-loop. Mutation of this residue in the small G-protein Ras results in the stabilization of its nucleotide-free form relative to both its GDP- and GTP-bound forms (14). This yields a Ras protein that has an enhanced affinity for Ras-guanine nucleotide exchange factors (Ras-GEFs) and thereby has been used as a dominant-negative inhibitor of signaling by endogenous Ras in cells. Mutations of this residue have also been performed in some Gα subunits. In the case of $G\alpha_o$ or $G\alpha_{i2}$, such changes resulted in their having an enhanced affinity for the Gβγ subunit complex (15, 16). A similar mutation in $G\alpha_S$ gave rise to an enhanced affinity for the β-adrenergic receptor (17).

In this study, we have changed the conserved serine residue in the P-loop of α_T* to an asparagine residue (S43N). This mutant, unlike wild-type α_T*, is able to undergo GDP-GTP exchange at a significant rate even in the absence of R*. Similar to the phenotype shown by the $G\alpha_S$ mutant toward the β-adrenergic receptor, the α_T*(S43N) mutant, when in the GDP-bound state, slows R*-stimulated GDP-GTP exchange upon wild-type α_T*. In addition, we show that the GTPγS-bound form of α_T*(S43N) is capable of activating the PDE and of slowing R*-stimulated GDP-GTP exchange upon wild-type α_T*. Moreover, using the activation of PDE as a probe, we have been able to show that GTPγS-bound α_T*(S43N) stabilizes what may represent an intermediate complex that forms along the G-protein activation pathway and consists of both R* and the β1γ1 subunit complex, together with the α_T subunit.

During the course of our studies, Artemyev and co-workers (18) reported the characterization of the same mutation within the chimeric α_T* subunit. However, they reported that α_T*(S43N) was not capable of undergoing an exchange of GTP for GDP. We believe that this was likely due to a step in their purification protocol that was carried out at room temperature that would have resulted in the loss of the bound nucleotide. We have indeed observed that prolonged incubation of the α_T*(S43N) mutant at room temperature renders it unable to bind GTPγS, and while it is still capable of binding to R* and preventing it from activating wild-type α_T*, it no longer exhibits many of the features that we describe below.

EXPERIMENTAL PROCEDURES

Materials—Frozen dark-adapted bovine retina were obtained from Lawson (Lincoln, NE). All other chemicals were from Sigma.

Purification of Visual Transduction Proteins—Rod outer segment (ROS) membranes were isolated as described (19). Holotransducin and PDE were obtained from ROS membranes essentially as described (20). The PDE was further purified by gel filtration chromatography on a HiLoad Superdex 200 HR26/60 column (GE Healthcare) equilibrated with HMAG buffer (20 mM Na-HEPES, pH 7.5, 5 mM $MgCl_2$, 1 mM Na-azide, and 10% glycerol). Urea-washed disc membranes were prepared as described and served as the source of R* (21).

Purification of the β1γ1 Complex—Holo-transducin was applied to two 5-ml Hitrap Blue-Sepharose columns (GE Healthcare), connected in tandem, that had been pre-equilibrated in G1G0A buffer (10 mM Na-HEPES, pH 7.5, 6 mM $MgCl_2$, 1 mM DTT, and 10% glycerol). The columns were first washed with 250 ml of G1G0A buffer. This was followed by a 250 ml of low salt wash (G1G0A buffer + 100 mM KCl) to elute the β1γ1 complex. The α_T subunit was then eluted with 250 ml of high salt buffer (G1G0A buffer + 500 mM KCl). The β1γ1 subunit complex was further purified by ion exchange chromatography using a 5-ml Hitrap Q-Sepharose column by applying a NaCl gradient (0–500 mM, 150 ml) in HMAG buffer (20 mM Na-HEPES, pH 7.5, 5 mM $MgCl_2$, 1 mM Na-azide, and 10% glycerol). The β1γ1 complex eluted at a salt concentration of ~100 mM and was then concentrated, flash-frozen, and stored at −80 °C.

*Expression and Purification of α_T**—We have used a construct designated pHis6Chi8, which was obtained from Dr. Heidi Hamm (Vanderbilt University). This chimera has the corresponding region from α_{i1} inserted between residues 215 and 295 of α_T. In addition, residues 244 and 247 were changed back to the original amino acids in α_T, yielding what we refer to as α_T*. The recombinant α_T* subunits, both wild-type and S43N, were expressed in BL21 (DE3) supercompetent cells and purified as described (11, 13). The proteins were further purified by ion exchange chromatography as outlined for the β1γ1 complex. The proteins were concentrated, aliquoted, snap-frozen, and stored at −80 °C. The final yield of chimeric α_T* was typically ~1–2 mg of pure protein/liter of bacterial culture. Nucleotide occupancy of the purified recombinant α_T* and α_T*(S43N) was determined using HPLC (11).

Determination of Active Concentrations of α_T Subunits*—The amount of active, functional α_T* was determined by assaying [^{35}S]GTPγS binding activity. Rhodopsin was light activated (R*) by incubation in ambient light for 5 min on ice. The α_T* subunits (500 nM) were incubated in the presence of 50 nM R*, 500 nM β1γ1, and 50 μM [^{35}S]GTPγS, in HMDM buffer (20 mM HEPES, pH 7.5, 5 mM $MgCl_2$, and 0.01% (w/v) dodecylmaltoside) at a total volume of 100 μl, for 1–2 h at room temperature. Subsequently, 40-μl aliquots were applied, in duplicate, to prewet nitrocellulose filters (Schleicher & Schuell, pore size, 0.45 μm) on a suction manifold. The filters were washed twice with HM buffer (20 mM HEPES, pH 7.5, 5 mM $MgCl_2$), added to scintillation liquid (30% LSC Scintisafe Mixture), and counted in a scintillation counter (LS6500 multipurpose scintillation counter). All protein concentrations of α_T* were determined by this procedure.

Time Course of GTPγS Binding—R* and β1γ1 were mixed with [^{35}S]GTPγS to give a final GTPγS concentration of 50 μM in HMDM buffer. The GDP-GTP exchange reaction was initiated by the addition of α_T*, with the final volume of the reaction mixture being 300 μl. At different times, 20-μl aliquots were added to prewetted nitrocellulose filters and processed as described in the previous section.

Fluorescence Measurements—Fluorescence measurements were carried out using a Varian eclipse spectrofluorimeter. The

binding of aluminum fluoride (AlF_4^-) was measured by monitoring the intrinsic tryptophan fluorescence of α_T* (excitation: 280 nm; emission: 340 nm). α_T* (300 nM) was mixed with 1 ml of HMDM buffer at room temperature and the tryptophan fluorescence emission was monitored continuously for 1 min. Subsequently, AlF_4^- (final concentrations: 5 mM NaF and 100 μM $AlCl_3$) was added while monitoring the tryptophan fluorescence emission in real-time.

GTPγS binding to α_T* was monitored by premixing R* (prepared as described above) and β1γ1 in HMDM buffer containing GTPγS (50 μM) and monitoring tryptophan fluorescence (excitation: 300 nm; emission: 345 nm) in real-time. Subsequently, α_T* (300 nM) was added. All kinetic traces were corrected for the fluorescence from R* and β1γ1.

The inhibition of GDP-GTP exchange upon α_T*(wild-type) by the GDP-bound form of α_T*(S43N) was measured by monitoring the kinetics of GTPγS binding using tryptophan fluorescence. This was carried out with 300 nM α_T*(wild-type), R* (5 nM), β1γ1 (300 nM), 50 μM GTPγS, and varying concentrations of α_T*(S43N).

The GTPγS-bound form of α_T*(S43N) was prepared by incubating the protein (5 μM) with 100 μM GTPγS in HMDM buffer at room temperature for 2 h. The protein was subsequently placed on ice. α_T*(S43N)-GTPγS was added at varying concentrations to a cuvette containing a mixture of R* (5 nM), β1γ1 (300 nM), and GTPγS (50 μM). Tryptophan fluorescence was monitored for 1 min and α_T*(wild-type) was added, and the kinetics of GTPγS binding were monitored. All kinetic data were fitted to a single exponential Equation 1,

$$F = F_\infty - (F_\infty - F_0)\exp(-k_{obs}t) \quad \text{(Eq. 1)}$$

where F = fluorescence signal at any time t, F_0 = fluorescence signal at time $t = 0$, F_∞ = fluorescence signal at $t = \infty$, k_{obs} = observed rate constant.

Labeling the β1γ1 Subunit Complex—The β1γ1 complex (10 μM) was incubated in a buffer containing 20 mM Na-HEPES (pH 7.5) and 5 mM $MgCl_2$ with a 0.5 mM solution of 5-((((2-iodoacetyl)amino)ethyl)amino)naphthalene-1-sulfonic acid (IAEDANS), dissolved in dimethyl formamide, at room temperature in the dark for 2 h. The reaction was quenched by the addition of β-mercaptoethanol at 11.2 mM. The labeled β1γ1 was separated from free probe and exchanged into HMAG buffer on a PD-10 desalting column (Amersham Biosciences). The extent of incorporation of the IAEDANS moiety was calculated using an extinction coefficient of 5600 M^{-1} cm^{-1} at 336 nm. The stoichiometry of labeling was determined by correcting the absorbance at 280 nm for IAEDANS absorption and measuring the concentration of β1γ1 using the calculated extinction coefficient of 53,600 M^{-1} cm^{-1}. The stoichiometry of labeling was determined to be 1.2 ± 0.1 mol per mol β1γ1.

Fluorescence Anisotropy Measurements—Anisotropy measurements of IAEDANS-labeled β1γ1 complexes were carried out on a Cary eclipse spectrofluorimeter in the L-format. All reported anisotropy values have been corrected by determination of G-factors using horizontally polarized light. The excitation and emission wavelengths were set at 336 nm (bandwidth = 10 nm) and 490 nm (bandwidth = 20 nm), respectively. An integration time of 10 s was used for all measurements.

Measurements of cGMP PDE Activity—The analysis of cGMP hydrolysis by the retinal PDE was carried out as described (22). Briefly, a pH microelectrode was used to measure the decrease in pH resulting from the production of a proton for each molecule of cGMP hydrolyzed by PDE. All assays were carried out at 22 °C in a final volume of 300 μl containing 5 mM HEPES (pH 7.4), 100 mM NaCl, and 2 mM $MgCl_2$ (AB buffer). The dose response for the activation of PDE by α_T* was determined by mixing R* (118 nM), β1γ1 (370 nM), 100 μM GTPγS, and α_T* in AB buffer. This mixture was incubated at room temperature for 1–2 h. PDE (70 nM) was added and incubated at room temperature for 5 min. The reaction was initiated by the addition of 2 mM cGMP. At the end of each assay period, the buffering capacity (in mV/nmol) was determined by adding 500 nmol of sodium hydroxide. The rate of hydrolysis of cGMP (nmol/s) was determined from the ratio of the initial slope of the pH record (mV/nmol) and the buffering capacity of the assay buffer (mV/nmol).

GTPγS-bound α_T*(S43N) was prepared by incubating the α_T* subunit (5 μM) with GTPγS (100 μM) in AB buffer for 2 h at room temperature. To determine the effects of R* and the β1γ1 subunit complex on PDE activation, R* and/or β1γ1 were mixed with GTPγS-bound α_T*(S43N), diluted in AB buffer containing 100 μM GTPγS to a final concentration of 250 nM, and incubated at room temperature for 5 min. PDE and cGMP were added to this mixture and the PDE activity measured as described above.

RESULTS

The Purified Recombinant α_T(S43N) Mutant Is Isolated with Bound GDP*—Both the Gα subunits of large G-proteins and the Ras-related small G-proteins bind to GDP with a very high affinity. This explains the requirement for an activated GPCR or a GEF to catalyze the dissociation of GDP from Gα subunits and Ras-related G-proteins, respectively, in order for GDP-GTP exchange to occur. In the case of the small G-proteins, the highly conserved serine/threonine residues in the P-loop help to coordinate Mg^{2+}, which is essential for the high affinity binding of GDP, such that substitutions at this site yield nucleotide-depleted, dominant-negative mutants (14). Magnesium is not necessary for the high affinity binding of GDP to the Gα subunits of large G-proteins, possibly because of their helical domain, which is lacking in the small G-proteins (23). However, the x-ray crystal structure of the GDP-bound form of α_T shows that the main-chain nitrogen of the serine residue at position 43 makes a hydrogen bond with one of the non-bridging oxygens on the β-phosphate of GDP, thereby suggesting a potentially important role in high-affinity binding (24). In addition, there have been suggestions that substitutions for the conserved P-loop serine/threonine residue in Gα subunits yield dominant-negative inhibitors, raising the question of whether these mutants are also nucleotide-depleted (16–18, 25–27). Thus, we performed HPLC analysis to determine whether the α_T*(S43N) mutant, following its purification, still contained bound guanine nucleotide. We found that as in the case for the wild-type α_T* subunit, the α_T*(S43N) mutant was purified with stoichio-

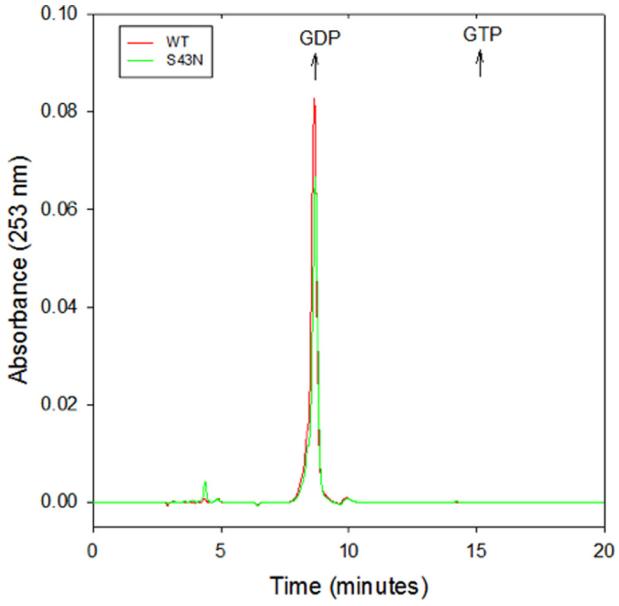

FIGURE 1. **HPLC analysis of the nucleotide occupancy of wild-type α_T* and α_T* (S43N).** Wild-type α_T* (*red*) and α_T*(S43N) (*green*) at concentrations of 100 μM were incubated in the presence of 7.5% acetonitrile for 5 min at room temperature and centrifuged at 16,000 × *g* for 10 min at room temperature. An aliquot of the supernatant (20 μl) was injected into a C18 reverse phase HPLC column equilibrated with 100 mM KH_2PO_4, pH 6.5, 10 mM tetrabutylammonium bromide, 0.2% NaN_3, and 7.5% acetonitrile, and then isocratic elution was performed. The absorbance at 253 nm was monitored. The elution times of GDP and GTP standards are indicated by *arrows*.

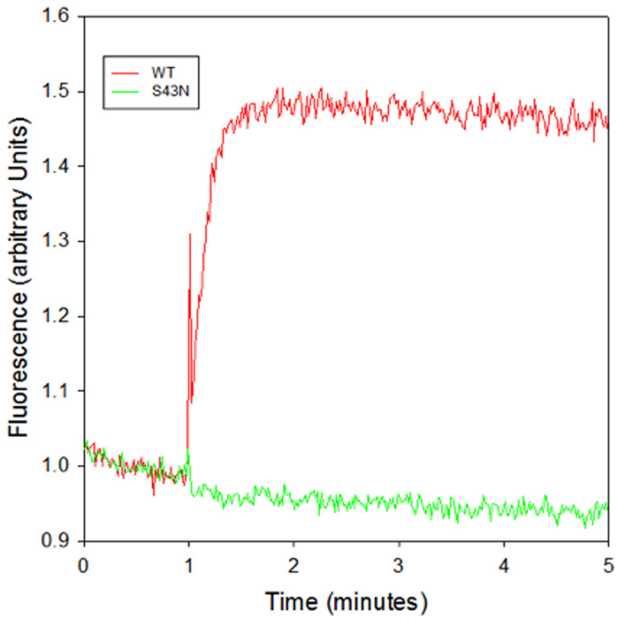

FIGURE 2. **AlF_4^- response of wild-type α_T* and α_T* (S43N).** Wild-type α_T* (*red*) and α_T*(S43N) (*green*) were incubated in HMDM buffer. At the indicated time, 20 μl of a premixed aliquot containing 250 mM NaF and 150 μM $AlCl_3$ to generate AlF_4^- was added and the enhancement in tryptophan fluorescence (excitation: 280 nm; emission: 340 nm) was monitored.

metric amounts of bound GDP (Fig. 1), *i.e.* with stoichiometries of 1 ± 0.1 mol GDP per mol α_T* and 0.8 ± 0.1 mol GDP per mol α_T*(S43N).

The x-ray crystal structure for the aluminum fluoride (AlF_4^-)/GDP-bound form of α_T shows that AlF_4^- occupies the γ-phosphate-binding site of GTP (28). This structure has been postulated to resemble the transition state for GTP hydrolysis. When AlF_4^- binds to the GDP-bound form of α_T, there is an increase in the intrinsic tryptophan fluorescence due to a conformational change in the Switch 2 region, one of three regions of α_T that change conformation upon binding GTP (29). As expected, a robust increase in tryptophan fluorescence was observed upon addition of AlF_4^- to the wild-type α_T* subunit (Fig. 2). However, the addition of AlF_4^- to the α_T*(S43N) mutant did not cause a detectable change in tryptophan fluorescence. This was not entirely unexpected since the presence of Mg^{2+} is required for the AlF_4^--induced enhancement in tryptophan fluorescence. The x-ray crystal structures of both the GTPγS- and AlF_4^--bound forms of α_T show that the side-chain hydroxyl oxygen of Ser-43 is one of the coordination sites for the bound divalent cation (Mg^{2+} in the GTPγS-bound α_T structure and Ca^{2+} in the AlF_4^--bound α_T structure) (28, 30). Thus, the α_T*(S43N) mutant would have a reduced affinity for Mg^{2+} and, consequently, might not be able to undergo the AlF_4^--induced conformational change that alters the position of Switch 2 and enhances its intrinsic tryptophan fluorescence.

R Has Only Minor Effects on GDP-GTP Exchange within the α_T*(S43N) Mutant*—Wild-type α_T* undergoes very slow guanine nucleotide exchange when assayed in the absence of R* and $\beta1\gamma1$, as monitored by either the enhancement in the intrinsic tryptophan fluorescence that accompanies the exchange of GDP for GTPγS (k_{obs} = 0.01 min^{-1}), or by using a filter binding assay to measure the exchange of GDP for [^{35}S]GTPγS (0.02 min^{-1}) (Fig. 3*A*, *open squares*). This is similar to the spontaneous nucleotide exchange rate reported earlier (31). In contrast, we found that the α_T*(S43N) mutant undergoes nucleotide exchange with a rate constant that is about 4–8-fold faster than that for the wild-type α_T* subunit (k_{obs} = 0.09 min^{-1}) as monitored using intrinsic tryptophan fluorescence (Fig. 3*A*, *dotted line*). A similar rate constant was obtained when using a filter binding assay to measure the exchange of GDP for [^{35}S]GTPγS (k_{obs} = 0.08 min^{-1}). A filter binding assay was used to measure the rate of dissociation of GDP using wild-type α_T* or α_T*(S43N) that had been preloaded with [^{3}H]GDP. This experiment showed that the rate of release of GDP from α_T*(S43N) was 4-fold faster than that of wild-type α_T* (Fig. 3*A*, *inset*). Thus, changing the serine to asparagine at position 43 within the α_T* subunit apparently causes a change in the conformation of the P-loop such that there is an increase in the rate of GDP dissociation, which has been suggested to be the rate-limiting step for GDP-GTP exchange (32).

When R* was added together with the $\beta1\gamma1$ subunit complex to wild-type α_T*, there was the expected marked increase in the rate of GDP-GTP exchange. For example, the addition of 12 nM R*, along with 300 nM $\beta1\gamma1$, to 300 nM wild-type α_T* increased the rate constant for guanine nucleotide exchange by at least 500-fold (Fig. 3*B*, *inset*, *open triangles*). This rate enhancement due to light-activated rhodopsin is similar to what has been reported earlier (10). However, the addition of even relatively high levels of R* to the α_T*(S43N) mutant had only minimal effects on the rate of nucleotide exchange (Fig. 3*B*). Specifically, when the α_T*(S43N) mutant was assayed in the presence of 112 nM R* and 400 nM $\beta1\gamma1$, the rate constant for GDP-GTP

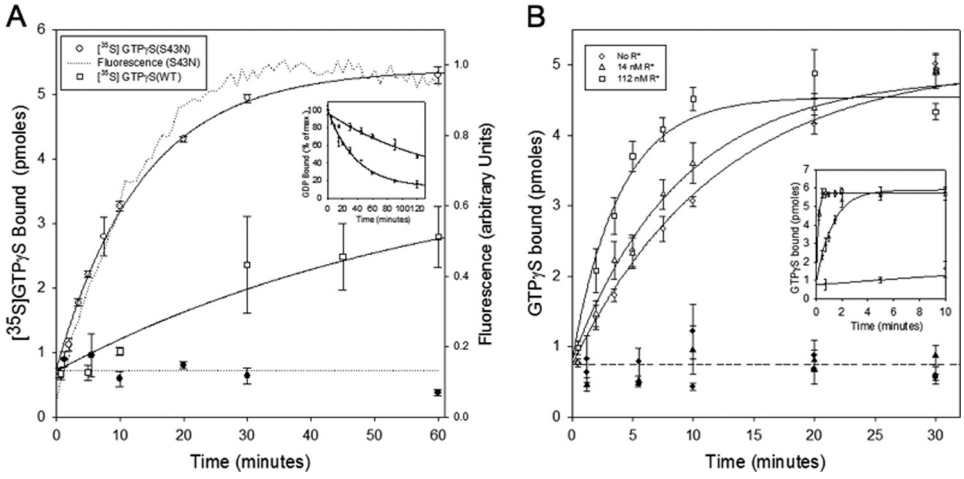

FIGURE 3. **The R*-independent and R*-dependent GDP-GTP exchange activity of α_T* (S43N).** *A*, 50 μM GTPγS or [^{35}S]GTPγS was added to 300 nM α_T*(S43N) or wild-type α_T*. In the case of GTPγS (dotted: α_T*(S43N)), the tryptophan fluorescence emission was monitored in real-time with the excitation wavelength set at 300 nm and the emission wavelength at 345 nm. When assaying [^{35}S]GTPγS binding to either α_T*(S43N) (○) or wild-type α_T* (□), aliquots (20 μl) of the reaction mixture were removed at the indicated times and added directly to pre-wetted nitrocellulose filters on a suction manifold to quench the reaction. The filters were subsequently washed twice with HM buffer and added to 3 ml of scintillation fluid and counted on a scintillation counter. The *y*-axis shows the number of pmol of GTPγS in 20 μl of the filtered reaction mix. The radioactivity data is shown as mean ± S.E. of three independent experiments. A combined single exponential fit (*solid line*) of all 3 data sets for α_T*(S43N) yielded a rate constant of 0.076 ± 0.005 min^{-1} (± S.E.). A single exponential fit of the fluorescence data for α_T*(S43N) yielded a rate constant of 0.085 ± 0.003 min^{-1} (mean ± S.E.; n = 21). Data from experiments carried out in the absence of α_T*(S43N) or wild-type α_T* are shown as closed circles. *Inset*, α_T*(S43N) or wild-type α_T* (5 μM) was incubated in the presence of 100 μM [^{3}H]GDP for either 2 or 3 h, respectively. The mixtures were diluted 10-fold into HM buffer containing 1 mM GTPγS and incubated at room temperature. At different times, aliquots (20 μl) of the reaction mixture were removed and treated as described above. The *y*-axis shows the percentage of [^{3}H]GDP remaining bound to the α_T* subunits, relative to the amount bound after 15 s of incubation. Wild-type α_T*: □. α_T*(S43N) : ○. *B*, 50 μM [^{35}S]GTPγS was added to 300 nM α_T*(S43N) in the presence of 400 nM $\beta1\gamma1$ and the indicated concentrations of R* (○: no R*; △: 14 nM R*; □: 112 nM R*). The samples were filtered and counted as described in *panel A*. The *y*-axis shows the number of pmol of GTPγS in 20 μl of the reaction mix. The radioactivity data are shown as mean ± S.E. of 3 independent experiments. Data from experiments carried out in the absence of α_T*(S43N) are shown as corresponding *closed symbols*. *Inset*, 50 μM [^{35}S]GTPγS was added to 300 nM wild-type α_T* in the presence of 400 nM $\beta1\gamma1$ and the indicated concentrations of R* (○: no R*; △: 14 nM R*; □: 112 nM R*). The samples were filtered and counted as described in *panel A*.

exchange was increased by only ~3-fold. The rate of GDP-GTP exchange upon wild-type α_T* was too fast to be measured under these conditions (Fig. 3*B*, *inset*, *open squares*). These findings suggested either that the α_T*(S43N) mutant is impaired in its ability to interact with R* or that the release of R* from the activated, GTPγS-bound mutant is slow relative to its rate of release from wild-type α_T*, thus compromising the ability of R* to act catalytically.

The β1γ1 Subunit Complex Has No Effect on the GDP-GTP Exchange Activity of the α_T (S43N) Mutant*—The $\beta1\gamma1$ subunit complex has been shown to increase the affinity of GPCRs like R* for their Gα-signaling partners, as well as to help GPCRs to further increase the rate of G-protein activation (33–37). The stimulatory actions of the $\beta1\gamma1$ subunit complex were clearly evident when assaying nucleotide exchange on the wild-type α_T* subunit, as the rate constant for R*-stimulated GDP-GTP exchange increased from 0.02 min^{-1} in the absence of $\beta1\gamma1$ to 0.78 min^{-1} in the presence of 400 nM $\beta1\gamma1$ (Fig. 4*A*, *inset*). This rate enhancement, due to the $\beta1\gamma1$ complex, is similar to that reported in earlier studies (10). However, this was not the case when assaying the α_T*(S43N) mutant, as the rate of nucleotide exchange upon the addition of 400 nM $\beta1\gamma1$ to α_T*(S43N) in the presence of 14 nM R* was 0.11 min^{-1} (Fig. 4*A*), similar to the rate constant obtained in the absence of $\beta1\gamma1$ (0.11 min^{-1}). Similarly, the $\beta1\gamma1$ subunit complex had no effect on the GDP-GTP exchange activity of the S43N mutant in the absence of R* (Fig. 4*B*). These findings raised the possibility that the α_T*(S43N) mutant might not be able to effectively interact with the $\beta1\gamma1$ subunit complex. We then used a fluorescence anisotropy assay that allows for the direct monitoring of the binding of Gα subunits to the $\beta1\gamma1$ subunit complex labeled with IAEDANS, and found that the α_T*(S43N) mutant bound to $\beta1\gamma1$ with an affinity that was similar to that for the binding of wild-type α_T* to $\beta1\gamma1$ (Fig. 4*C*). This indicates that the $\beta1\gamma1$ subunit complex is able to bind to the α_T*(S43N) mutant but it is unable to help accelerate the nucleotide exchange reaction in the presence of R*.

As expected, the rate of R*-stimulated GDP-GTP exchange on wild-type α_T* was very slow in the absence of any added $\beta1\gamma1$. However, the rate of GDP-GTP exchange was enhanced in the presence of 60 nM $\beta1\gamma1$. Importantly, a similar rate of GDP-GTP exchange was observed when the IAEDANS-labeled $\beta1\gamma1$ was used instead of unlabeled $\beta1\gamma1$ (Fig. 4*C*, *inset*), demonstrating that the IAEDANS-labeled $\beta1\gamma1$ was functionally equivalent to its unlabeled counterpart.

α_T (S43N) Slows the Rate of R*-dependent GDP-GTP Exchange on Wild-type α_T**—It was first shown for the small G-protein Ras, that changing the serine residue at position 17, corresponding to Ser-43 in α_T*, to asparagine (S17N) yielded a potent dominant-negative inhibitor of Ras signaling by sequestering upstream GEFs (38, 39). Likewise, the α_T*(S43N) mutant, even at relatively low concentrations in comparison to wild-type α_T*, was able to inhibit R*-stimulated GDP-GTP exchange on the wild-type α_T* subunit (Fig. 5*A*, *inset*). Specifically, the addition of ~20 nM α_T*(S43N) slowed the rate of R*-stimulated nucleotide exchange on wild-type α_T* (300 nM) by ~70-fold (Fig. 5*A*), indicating that the GDP-bound form of

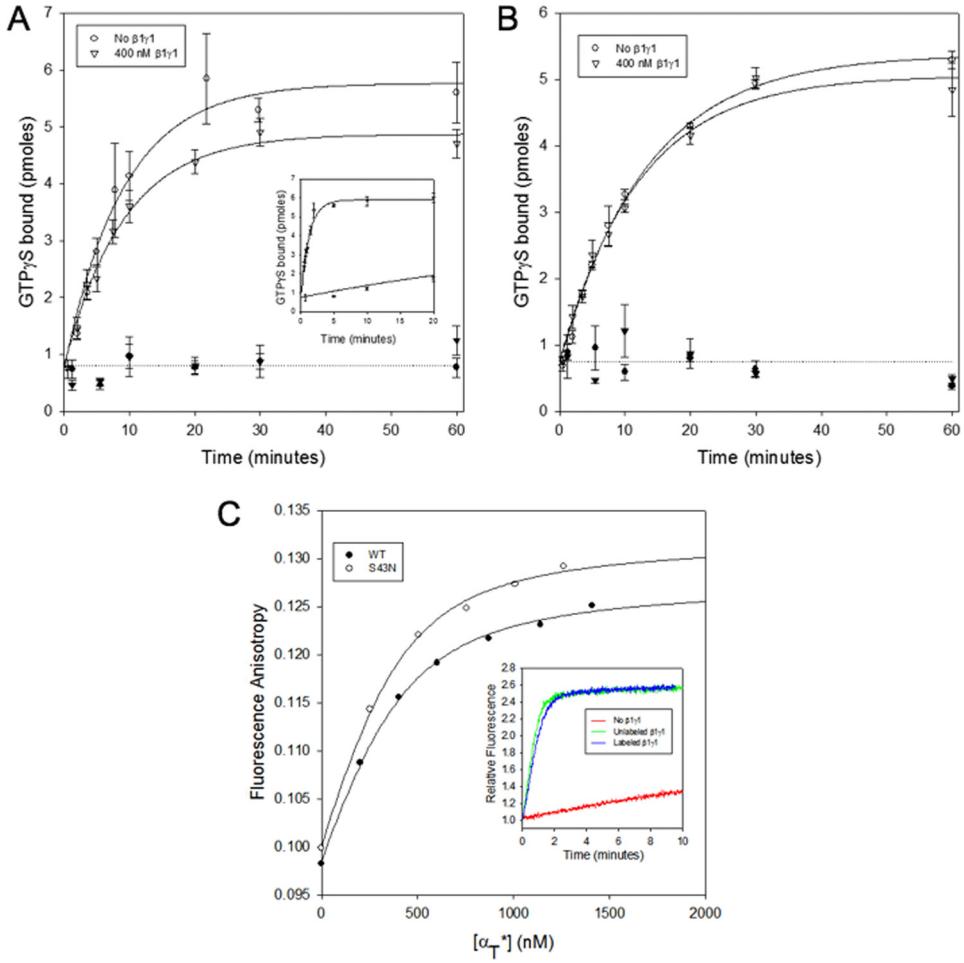

FIGURE 4. **Effects of $\beta1\gamma1$ on the GDP-GTP exchange activity of α_T* (S43N).** *A*, 50 μM [^{35}S]GTPγS was added to 300 nM α_T*(S43N) and 14 nM R* in the absence (○) or presence of 400 nM $\beta1\gamma1$ (▽). The samples were filtered and counted as described in the legend for Fig. 3*A*. The radioactivity data is shown as the mean ± S.E. of three independent experiments. The *lines* through the data show a simultaneous single exponential fit of all 3 data sets. Data from experiments carried out in the absence of α_T*(S43N) are shown as corresponding *closed symbols*. *Inset*, 50 μM [^{35}S]GTPγS was added to 300 nM wild-type α_T* and 14 nM R* in the absence or presence of 400 nM $\beta1\gamma1$. The samples were filtered and counted as described in the legend for Fig. 3*A*. *B*, 50 μM [^{35}S]GTPγS was added to 300 nM α_T*(S43N) in the absence (○) or presence of 400 nM $\beta1\gamma1$ (▽). The samples were filtered and counted as described in the legend for Fig. 3*A*. The *y*-axis shows the number of pmol of GTPγS in 20 μl of the reaction mix. The radioactivity data is shown as the mean ± S.E. of three independent experiments. The lines through the data show a simultaneous single exponential fit of all 3 data sets. Data from experiments carried out in the absence of α_T*(S43N) are shown as corresponding closed symbols. *C*, aliquots of wild-type α_T* (○) and α_T*(S43N) (●) were added successively to the $\beta1\gamma1$ complex (400 nM) labeled with IAEDANS in HMDM buffer and the fluorescence anisotropy was monitored (excitation = 336 nm, emission = 490 nm). The data were fit to a bimolecular binding model. *Inset*, 50 μM GTPγS was added to 300 nM wild-type α_T* and 10 nM R* in the absence (*red line*) or the presence of either 60 nM unlabeled $\beta1\gamma1$ complex (*green*), or the $\beta1\gamma1$ complex labeled with IAEDANS (*blue line*) in HMDM buffer, and the tryptophan fluorescence emission was monitored in real-time with the excitation wavelength set at 300 nm and the emission wavelength at 345 nm.

α_T*(S43N) was able to bind to R* with high affinity and prevent it from binding and activating the wild-type α_T* subunit.

Interestingly, we found that the GTPγS-bound form of the α_T*(S43N) mutant was also capable of forming a stable complex with R*. As shown in Fig. 5*B*, increasing concentrations of the GTPγS-bound form of this α_T* mutant were able to reduce the rate of R*-stimulated GDP-GTP exchange on wild-type α_T*. For example, the addition of ~50 nM GTPγS-bound α_T*(S43N) slowed the rate of GDP-GTP exchange on wild-type α_T* by ~10-fold (Fig. 5*B*, *inset*).

Addition of light-activated rhodopsin at 115 nM was able to relieve the inhibition of nucleotide exchange on wild-type α_T* caused by the addition of either GDP-bound (Fig. 5*C*) or GTPγS-bound (Fig. 5*D*) α_T*(S43N). This suggests the idea that the α_T*(S43N) mutant is acting by forming a stable complex with R* and blocking its interaction with wild-type α_T*.

R and the β1γ1 Subunit Complex Together Inhibit PDE Activation by α_T* (S43N)*—Given the indications that the GTPγS-bound α_T*(S43N) mutant can form a stable complex with R*, we were interested in seeing whether the α_T*(S43N)-GTPγS species was also capable of engaging and regulating the cyclic GMP PDE. We found that like GTPγS-bound wild-type α_T*, the GTPγS-bound α_T*(S43N) mutant was able to bind to the PDE and stimulate its activity in a dose-dependent manner (Fig. 6*A*). The activation of the PDE by wild-type α_T* was unaffected when R* and the $\beta1\gamma1$ subunit complex were added separately or together. This is because α_T*-GTPγS has a very low affinity for R* and $\beta1\gamma1$. Similarly, the ability of α_T*(S43N)-GTPγS to activate PDE was unaffected when R* and the $\beta1\gamma1$ complex were added individually to α_T*(S43N). However, surprisingly, the addition of R* and the $\beta1\gamma1$ subunit complex together to α_T*(S43N) inhibited its ability to activate the PDE (Fig. 6*B*). The

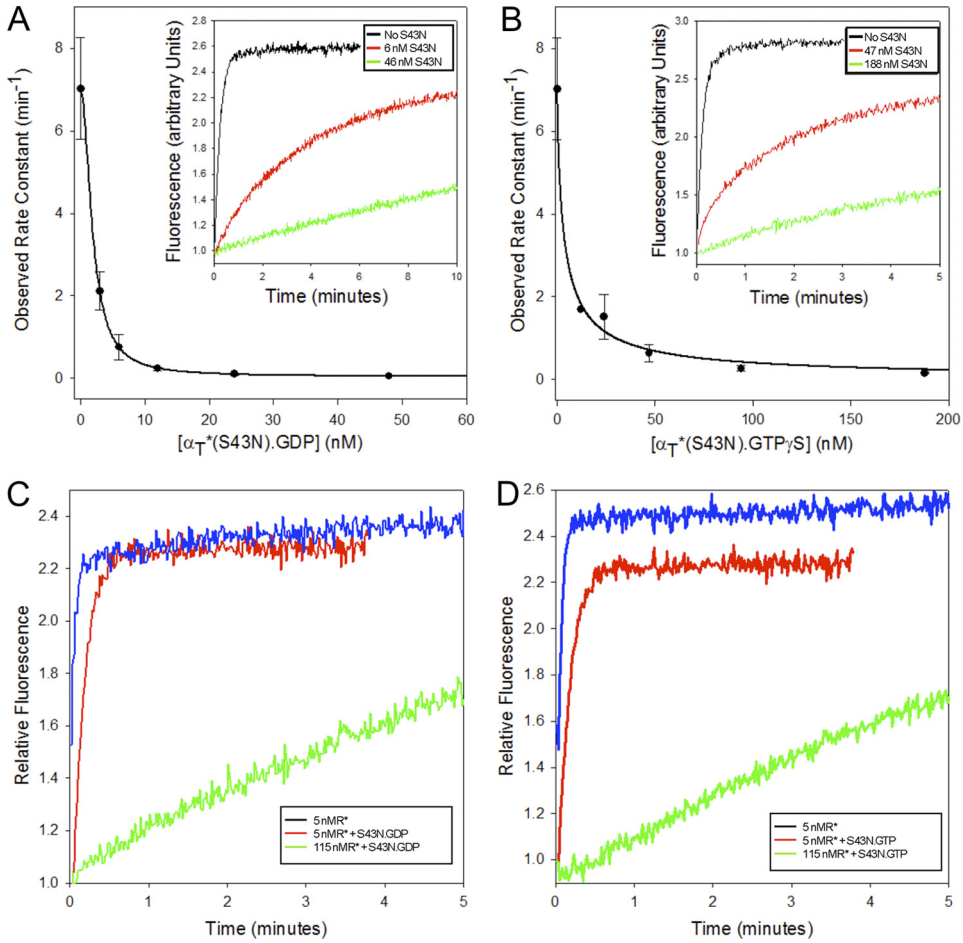

FIGURE 5. **Effects of α_T* (S43N) on the R*-dependent GDP/GTP exchange activity of wild-type α_T*.** *A*, 50 μM GTPγS was added to 6 nM R*, 300 nM wild-type α_T*, 300 nM β1γ1, and varying concentrations of α_T*(S43N) bound to GDP. The tryptophan fluorescence emission of the sample was monitored in real time with the excitation wavelength set at 300 nm and the emission wavelength set at 345 nm. Rate constants obtained from single exponential fits of the data are plotted as a function of the concentration of added α_T*(S43N). *Inset*: intrinsic tryptophan fluorescence is plotted as a function of time at different concentrations of α_T*(S43N) (*black*: none, *red*: 6 nM, *green*: 46 nM). *B*, 50 μM GTPγS was added to 6 nM R*, 300 nM wild-type α_T*, 300 nM β1γ1, and varying concentrations of α_T*(S43N) bound to GTPγS. The tryptophan fluorescence emission of the sample was monitored in real time with the excitation wavelength set at 300 nm and the emission wavelength set at 345 nm. Rate constants obtained from single exponential fits of the data are plotted as a function of the concentration of added α_T*(S43N). *Inset*: intrinsic tryptophan fluorescence is plotted as a function of time at different concentrations of α_T*(S43N) (*black*: none, *red*: 47 nM, *green*: 188 nM). *C*, 50 μM GTPγS was added to a mixture containing either 5 nM (*red* or *green line*) or 115 nM R* (*blue line*), 300 nM wild-type α_T*, 300 nM β1γ1, in the presence (*green* or *blue line*) or absence (*red line*) of 30 nM α_T*(S43N) bound to GDP. The tryptophan fluorescence emission of the sample was monitored in real time with the excitation wavelength set at 300 nm and the emission wavelength set at 345 nm. *D*, 50 μM GTPγS was added to a mixture containing either 5 nM (red or green line) or 115 nM R* (blue line), 300 nM wild-type α_T*, 300 nM β1γ1, in the presence (*green* or *blue line*) or absence (*red line*) of 100 nM α_T*(S43N) bound to GTPγS. The tryptophan fluorescence emission of the sample was monitored in real time with the excitation wavelength set at 300 nm and the emission wavelength set at 345 nm.

inhibition of the α_T*(S43N)-stimulated PDE activity occurred in a dose-dependent manner with respect to either R* (Fig. 7*A*) or the β1γ1 subunit complex (Fig. 7*B*). This suggests that R*, the activated form of α_T*(S43N), and the β1γ1 subunit complex are able to form a ternary complex that prevents α_T*(S43N) from stimulating PDE activity.

DISCUSSION

The visual phototransduction pathway has been proven to be a valuable system for understanding how a heptahelical GPCR can lead to the activation of its cognate G-protein and to the stimulation of an intracellular effector activity (40). However, despite an extensive number of biochemical and structural studies, the exact sequence of events that occurs during this process is not clear. According to the traditional model for G-protein activation, a GPCR that is activated by an external stimulus like light or hormones binds to a heterotrimeric G-protein. This binding triggers the release of GDP from the Gα subunit and its replacement by GTP. The binding of GTP has been shown to cause structural changes in the Gα subunit (24). These structural changes have been proposed to cause the dissociation of the Gα subunit from both the βγ subunit complex and the activated GPCR. The GTP-bound Gα subunit can then bind to and regulate its downstream targets.

Our strategy for gaining a better understanding of the mechanism of G-protein activation has been to identify and characterize Gα mutants that might provide insight into different stages of the activation process (10–12). In particular, we have generated mutations within a chimeric α_T subunit, referred to as α_T*, that contains an insertion between residues 215 and 295 of the corresponding region from $G\alpha_{i1}$. Although the insertion comprises 79 residues, there are only 21 amino acid substitu-

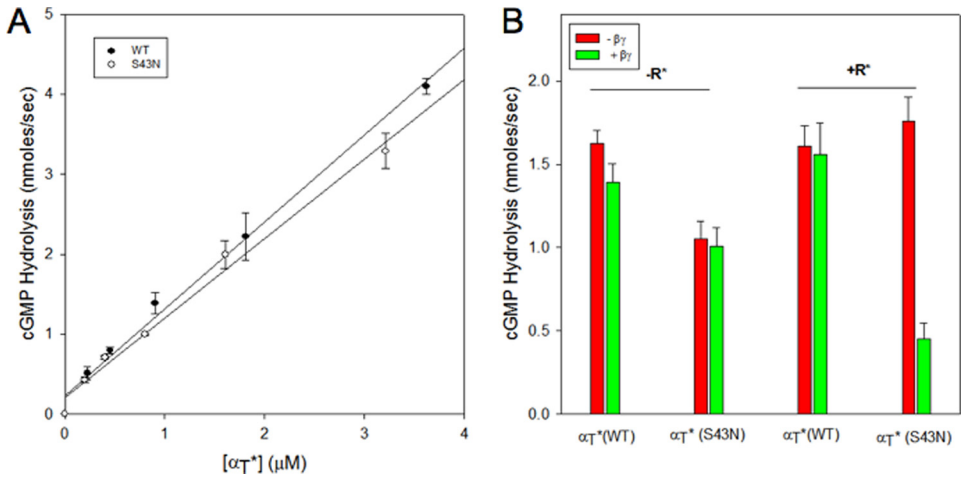

FIGURE 6. **PDE activation by α_T* (S43N).** *A*, wild-type α_T* (●) or α_T*(S43N) (○) at various concentrations was preincubated with 100 μM GTPγS in the presence of 118 nM R* and 370 nM $\beta1\gamma1$ for 1 h in a buffer containing 5 mM HEPES, pH 7.4 (AB buffer), at room temperature. PDE (70 nM) was added to this mixture and the pH of the sample was monitored. Subsequently, cGMP (2 mM) was added to initiate the reaction and the change in pH was monitored over time. At the end of the assay period, the buffering capacity (mV/nmol) was determined by the addition of 600 nmol of NaOH to the reaction mixture. The rate of hydrolysis of cGMP (nmol/s) was determined from the ratio of the slope of the pH record (mV/s) and the buffering capacity of the assay buffer (mV/nmol) and plotted on the Y-axis. The data are shown as the mean ± S.E. from three independent experiments. *B*, GTPγS-bound α_T*(S43N) or wild-type α_T* was prepared by incubating either α_T* subunit with 100 μM GTPγS at room temperature for 2 h and then placed on ice. The incubation mixture contained 1 μM R* and 1 μM $\beta1\gamma1$ in the case of wild-type α_T*. Subsequently, the GTPγS-bound α_T* subunits were diluted into AB buffer to a final concentration of 250 nM in the presence or absence of R* (4.8 μM) and $\beta1\gamma1$ (400 nM) and incubated at room temperature for 5 min. PDE was added to a final concentration of 160 nM, and its activation was measured as described for *panel A*. The data are presented as a bar graph with the *y*-axis showing the PDE activity in nmol/s. The *red bars* show data in the absence of $\beta1\gamma1$, and the *green bars* show data in the presence of $\beta1\gamma1$. The presence or absence of R* and the identity of the α_T* subunits are shown on the plots.

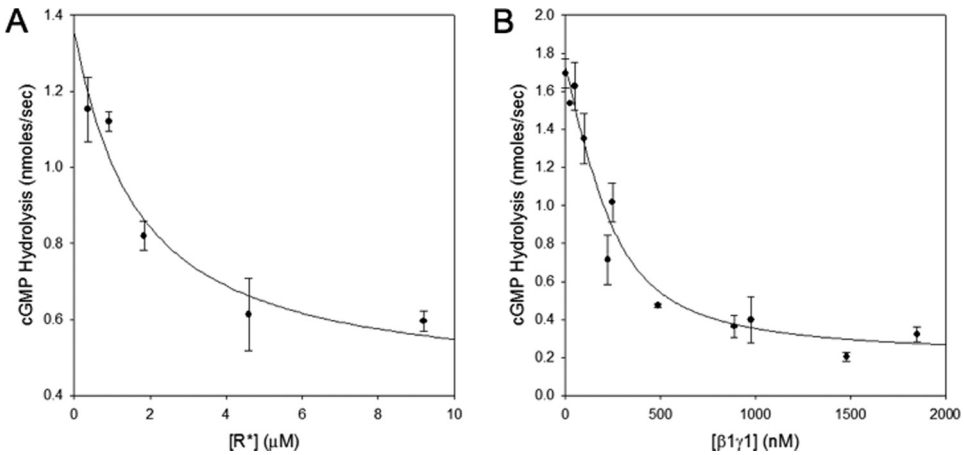

FIGURE 7. **Effects of R* and $\beta1\gamma1$ on PDE activation by α_T* (S43N).** α_T*(S43N) bound to GTPγS was prepared as described in Fig. 6*B*. This was diluted in AB buffer to a final concentration of 250 nM. Subsequently, the $\beta1\gamma1$ subunit complex (500 nM, *panel A*) or R* (4.8 μM, *panel B*) was added to the sample in the presence of varying concentrations of R* (*panel A*) or $\beta1\gamma1$ (*panel B*). PDE was added to a final concentration of 160 nM, and its activation was measured as described for Fig. 6*B*.

tions, of which 12 are conservative. This insertion includes the substitution of residues in the conformationally sensitive Switch 3 region of α_T. Despite these alterations, α_T* is similar to retinal α_T in undergoing GDP-GTP exchange in a R*-dependent manner and activating the cGMP phosphodiesterase.

In this study, we have changed the conserved serine residue within the region referred to as the P-loop to an asparagine residue. In the x-ray crystal structures of α_T, in complex with either GDP or GTPγS, the main-chain nitrogen of Ser43 forms a hydrogen bond with the non-bridging oxygen of the β-phosphate of the nucleotide (24, 30). In addition, the side-chain hydroxyl oxygen of Ser-43 forms hydrogen bonds with the carboxyl oxygen of Asp-196, located in the Switch 2 region, in both the GDP- and GTPγS-bound forms of α_T, and with the side-chain hydroxyl of Thr-177 in the GTPγS-bound structure of α_T.

One of the first observations we made regarding the α_T*(S43N) mutant was its ability to undergo spontaneous GDP-GTP exchange, in the absence of R*. The rate-limiting step of the GDP-GTP exchange reaction is the release of GDP from the α_T subunit (32). Thus, the S43N mutation apparently causes a change in the conformation of the P-loop to enhance the rate of GDP release. Still despite its weakened affinity, a substantial fraction of the purified α_T*(S43N) mutant contains bound GDP as indicated by reverse-phase HPLC.

Surprisingly, R* was much less effective at stimulating GDP-GTP exchange on α_T*(S43N) compared with the wild-type α_T* subunit. The main binding site for R* on the α_T subunit is

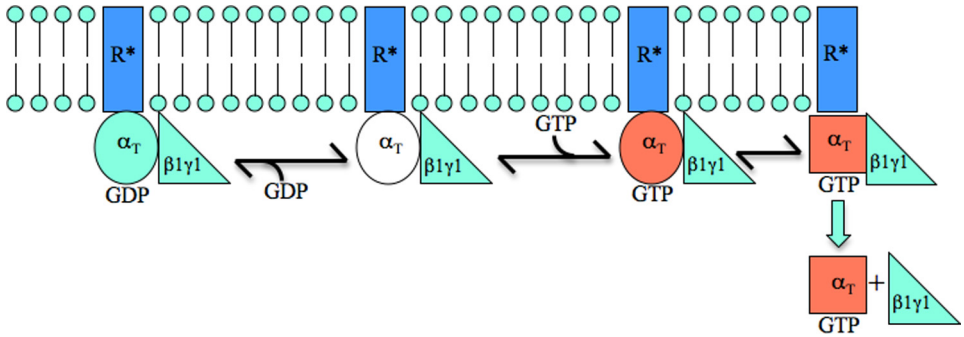

FIGURE 8. **The α_T* (S43N) mutant makes it possible to trap a GPCR-Gα-GTP-G$\beta\gamma$ complex.** The activation of a GPCR (*e.g.* R*) promotes its interaction with a heterotrimeric G-protein (α_T-GDP-$\beta1\gamma1$). This results in GDP-GTP exchange on α_T, leading to a conformational change (*i.e.* depicted by the change from a *red circle* to a *red square*) that enables α_T-GTP to dissociate from $\beta1\gamma1$ and R*. Apparently, the binding of Mg^{2+} by α_T is necessary for this conformational change. Thus, the GTP-bound α_T*(S43N) mutant, that is incapable of binding Mg^{2+} and undergoing such a conformational change, is able to form a stable complex with R* and $\beta1\gamma1$.

located at the C terminus, which is a considerable distance from the P-loop (4). This suggested that the impaired ability of R* to catalyze GDP-GTP exchange on α_T*(S43N) might not be due to R* having a reduced affinity for the GDP-bound form of α_T*(S43N). Instead, the α_T*(S43N) mutant may be impaired in its ability to undergo the necessary conformational change following GTP binding that enables a rapid release of R*, thereby making R* a less efficient catalyst of the nucleotide exchange reaction.

Mutation of the homologous serine residue in the monomeric G-protein Ras to an asparagine (S17N) yields a protein whose nucleotide-free form has an extremely high affinity for its GEFs (14, 38). Introduction of this mutant into cells inhibits the activation of wild-type Ras, such that it behaves as a dominant-negative inhibitor (38). Similar to the S17N mutant of Ras, the α_T*(S43N) mutant inhibits the activation of wild-type α_T*. Because GTPγS is able to bind to α_T*(S43N) in the absence of R*, we were able to prepare GTPγS-bound α_T*(S43N) and examine its effects on the GDP-GTP exchange activity of wild-type α_T*. We found that the GTPγS-bound form of α_T*(S43N) was also able to inhibit R*-dependent GDP-GTP exchange on wild-type α_T*, in a dose-dependent manner. These findings suggest that upon the binding of GTPγS, the α_T*(S43N) mutant was still capable of associating with the activated receptor.

GTPγS-bound wild-type α_T*, that was prepared in the presence of low concentrations of R* and $\beta1\gamma1$, activated the cGMP PDE very effectively. The presence of high concentrations of R* and $\beta1\gamma1$, either separately or together, had no effect on the ability of GTPγS-bound α_T* to activate the PDE. This is consistent with the observation that upon binding GTPγS, wild-type α_T* dissociates from R* and $\beta1\gamma1$ (41). The GTPγS-bound form of α_T*(S43N) is able to activate the cGMP PDE with a dose-response that is similar to that for wild-type α_T*. Neither the addition of R* alone, nor $\beta1\gamma1$ alone, had any effect on the activation of the PDE by GTPγS-bound α_T*(S43N). However, the combined addition of R* and $\beta1\gamma1$ strongly inhibited the activation of the PDE by α_T*(S43N). This provides evidence for the existence of a ternary complex consisting of R*, GTPγS-bound α_T*(S43N), and $\beta1\gamma1$. The existence of such a ternary complex was initially postulated based on the enhancement of the cholera toxin-catalyzed ADP-ribosylation of retinal α_T that was induced in the presence of R*, the $\beta1\gamma1$ subunit complex, and the non-hydrolyzable GTP analog Gpp(NH)p (42, 43). The ability of a ternary complex to form consisting of an activated receptor, an activated Gα subunit, and a G$\beta\gamma$ subunit complex carries interesting implications for the mechanisms that describe the reaction pathway for the activation of heterotrimeric G-proteins, as it raises important questions concerning whether G$\beta\gamma$ has a role in influencing the binding of GTP and the ensuing GTP-induced activating conformational change within Gα, as well as when the activated GTP-bound Gα subunit dissociates from G$\beta\gamma$ and the receptor, as this has been been traditionally assumed to be necessary for Gα to engage and regulate its effector activity.

Based on these findings, we propose the following model (Fig. 8). The exchange of GTP for GDP within a Gα subunit complexed to $\beta1\gamma1$ and R* leads to the formation of a ternary complex. We postulate that the α_T*(S43N) mutant stabilizes the ternary complex, such that it persists even following GDP-GTP exchange on α_T*(S43N). It has been shown that the binding of Mg^{2+} is essential for the enhancement in intrinsic trytophan fluorescence that accompanies the conformational change in Switch 2 that occurs upon the activation of retinal α_T (44). In the case of the α_T*(S43N) mutant, we observe changes in its intrinsic tryptophan fluorescence upon binding GTPγS, but these changes are substantially smaller than those for wild-type α_T*. The Switch 2 region is one of two regions on the α_T subunit, with the other being the N-terminal helix, that is involved in binding to the $\beta1\gamma1$ complex (45). This subunit complex has been shown to increase the affinity of α_T for R* (34). Thus, in order for GTP-bound α_T to dissociate from R*, the affinity of $\beta1\gamma1$ for α_T has to be reduced and this might be an outcome of a Mg^{2+}-induced conformational change that occurs in Switch 2. The inability of the GTP-bound α_T*(S43N) mutant to undergo this Mg^{2+}-dependent conformational change would then stabilize a ternary complex consisting of R*, α_T*(S43N)-GTPγS, and $\beta1\gamma1$. However, the free GTPγS-bound α_T*(S43N) species (*i.e.* when not associated with either R* or $\beta1\gamma1$) is able to activate the cGMP PDE as effectively as wild-type α_T*. This indicates that upon GDP-GTP exchange, α_T*(S43N) is able to couple to its biological effector (*i.e.* the PDE), provided that neither R* or $\beta1\gamma1$ is bound to this mutant so as to interfere with effector binding.

In summary, we have characterized an S43N mutant of a Gα subunit and shown that it can stabilize a ternary complex that also includes a GPCR (R*) and a Gβγ complex (β1γ1). Thus, the α_T*(S43N) acts as a dominant negative inhibitor of wild-type α_T by sequestering R* and β1γ1, even when it is bound to GTP. Perhaps more importantly, this α_T* mutant makes it possible to trap a previously uncharacterized intermediate along the G-protein activation pathway (*i.e.* consisting of the receptor, the GTP-bound Gα subunit, and the Gβγ complex).

Acknowledgments—We thank Cindy Westmiller for excellent secretarial assistance and Jon Erickson for comments on the manuscript.

REFERENCES

1. Kobilka, B., and Schertler, G. F. (2008) *Trends Pharmacol. Sci.* **29,** 79–83
2. Gether, U., and Kobilka, B. K. (1998) *J. Biol. Chem.* **273,** 17979–17982
3. Sprang, S. R., Chen, Z., and Du, X. (2007) *Adv. Protein Chem.* **74,** 1–65
4. Oldham, W. M., and Hamm, H. E. (2008) *Nat. Rev. Mol. Cell Biol.* **9,** 60–71
5. Oldham, W. M., and Hamm, H. E. (2007) *Adv. Protein Chem.* **74,** 67–93
6. Burns, M. E., and Arshavsky, V. Y. (2005) *Neuron* **48,** 387–401
7. Chen, C. K. (2005) *Rev. Physiol. Biochem. Pharmacol.* **154,** 101–121
8. Mittal, R., Erickson, J. W., and Cerione, R. A. (1996) *Science* **271,** 1413–1416
9. Li, Q., and Cerione, R. A. (1997) *J. Biol. Chem.* **272,** 21673–21676
10. Majumdar, S., Ramachandran, S., and Cerione, R. A. (2004) *J. Biol. Chem.* **279,** 40137–40145
11. Majumdar, S., Ramachandran, S., and Cerione, R. A. (2006) *J. Biol. Chem.* **281,** 9219–9226
12. Pereira, R., and Cerione, R. A. (2005) *J. Biol. Chem.* **280,** 35696–35703
13. Skiba, N. P., Thomas, T. O., and Hamm, H. E. (2000) *Methods Enzymol.* **315,** 502–524
14. John, J., Rensland, H., Schlichting, I., Vetter, I., Borasio, G. D., Goody, R. S., and Wittinghofer, A. (1993) *J. Biol. Chem.* **268,** 923–929
15. Slepak, V. Z., Quick, M. W., Aragay, A. M., Davidson, N., Lester, H. A., and Simon, M. I. (1993) *J. Biol. Chem.* **268,** 21889–21894
16. Slepak, V. Z., Katz, A., and Simon, M. I. (1995) *J. Biol. Chem.* **270,** 4037–4041
17. Cleator, J. H., Mehta, N. D., Kurtz, D. T., and Hildebrandt, J. D. (1999) *FEBS Lett.* **443,** 205–208
18. Natochin, M., Barren, B., and Artemyev, N. O. (2006) *Biochemistry* **45,** 6488–6494
19. Fawzi, A. B., and Northup, J. K. (1990) *Biochemistry* **29,** 3804–3812
20. Kroll, S., Phillips, W. J., and Cerione, R. A. (1989) *J. Biol. Chem.* **264,** 4490–4497
21. Min, K. C., Gravina, S. A., and Sakmar, T. P. (2000) *Protein Expr. Purif.* **20,** 514–526
22. Liebman, P. A., and Evanczuk, A. T. (1982) *Methods Enzymol.* **81,** 532–542
23. Higashijima, T., Ferguson, K. M., Sternweis, P. C., Smigel, M. D., and Gilman, A. G. (1987) *J. Biol. Chem.* **262,** 762–766
24. Lambright, D. G., Noel, J. P., Hamm, H. E., and Sigler, P. B. (1994) *Nature* **369,** 621–628
25. Cleator, J. H., Ravenell, R., Kurtz, D. T., and Hildebrandt, J. D. (2004) *J. Biol. Chem.* **279,** 36601–36607
26. Berlot, C. H. (2002) *J. Biol. Chem.* **277,** 21080–21085
27. Iiri, T., Bell, S. M., Baranski, T. J., Fujita, T., and Bourne, H. R. (1999) *Proc. Natl. Acad. Sci. U.S.A.* **96,** 499–504
28. Sondek, J., Lambright, D. G., Noel, J. P., Hamm, H. E., and Sigler, P. B. (1994) *Nature* **372,** 276–279
29. Phillips, W. J., and Cerione, R. A. (1988) *J. Biol. Chem.* **263,** 15498–15505
30. Noel, J. P., Hamm, H. E., and Sigler, P. B. (1993) *Nature* **366,** 654–663
31. Natochin, M., Granovsky, A. E., Muradov, K. G., and Artemyev, N. O. (1999) *J. Biol. Chem.* **274,** 7865–7869
32. Ferguson, K. M., Higashijima, T., Smigel, M. D., and Gilman, A. G. (1986) *J. Biol. Chem.* **261,** 7393–7399
33. Phillips, W. J., and Cerione, R. A. (1992) *J. Biol. Chem.* **267,** 17032–17039
34. Phillips, W. J., Wong, S. C., and Cerione, R. A. (1992) *J. Biol. Chem.* **267,** 17040–17046
35. Fawzi, A. B., Fay, D. S., Murphy, E. A., Tamir, H., Erdos, J. J., and Northup, J. K. (1991) *J. Biol. Chem.* **266,** 12194–12200
36. Wildman, D. E., Tamir, H., Leberer, E., Northup, J. K., and Dennis, M. (1993) *Proc. Natl. Acad. Sci. U.S.A.* **90,** 794–798
37. Jian, X., Clark, W. A., Kowalak, J., Markey, S. P., Simonds, W. F., and Northup, J. K. (2001) *J. Biol. Chem.* **276,** 48518–48525
38. Feig, L. A., and Cooper, G. M. (1988) *Mol. Cell. Biol.* **8,** 3235–3243
39. Feig, L. A. (1999) *Nat. Cell Biol.* **1,** E25–E27
40. Arshavsky, V. Y., Lamb, T. D., and Pugh, E. N., Jr. (2002) *Annu. Rev. Physiol.* **64,** 153–187
41. Fung, B. K. (1983) *J. Biol. Chem.* **258,** 10495–10502
42. Abood, M. E., Hurley, J. B., Pappone, M. C., Bourne, H. R., and Stryer, L. (1982) *J. Biol. Chem.* **257,** 10540–10543
43. Navon, S. E., and Fung, B. K. (1984) *J. Biol. Chem.* **259,** 6686–6693
44. Zelent, B., Veklich, Y., Murray, J., Parkes, J. H., Gibson, S., and Liebman, P. A. (2001) *Biochemistry* **40,** 9647–9656
45. Lambright, D. G., Sondek, J., Bohm, A., Skiba, N. P., Hamm, H. E., and Sigler, P. B. (1996) *Nature* **379,** 311–319